



Ionic liquids for pitting corrosion inhibition of aluminum alloy in saline-alkaline solution

H.M. El-Saeed^a, M.A. Deyab^b, K. Shalabi^a, Emad E.El-Katori^c, A.S. Fouda^{a*}

^a Department of Chemistry, Faculty of Science, Mansoura University, Mansoura 35516, Egypt.

^b Egyptian Petroleum Research Institute (EPRI), Nasr City 11727, Cairo, Egypt.

^c Department of Chemistry, Faculty of Science, New Valley University, El-Kharja 72511, Egypt.

* Email: asfouda@hotmail.com, Tel: +2 050 2365730

Received: 15/3/2022
Accepted: 25/4/2022

Abstract: Under different experimental settings, three liquids based on imidazolium were studied as green inhibitors for pitting corrosion of aluminum alloy (AA6061) in a saline-alkaline solution (1.0 M NaCl + 0.1M Na₂CO₃). This research uses cyclic polarization (CP), potentiodynamic polarization (PP), AC Impedance spectroscopy (EIS), and surface morphology. The inclusion of ionic liquids clearly altered the pitting potential to a more positive value. The size of both the capacitive and inductive loops in the EIS graphs expanded dramatically as the concentration of ionic liquids increased. Ionic liquids delay aluminum corrosion by adsorbing the compound to the alloy surface, according to SEM, AFM, XPS studies.

keywords: pitting corrosion; aluminum alloy; Ionic liquids, electrochemistry

1. Introduction

Aluminum is widely employed in a variety of industries, including automotive, aerospace, aviation, radiators, household goods, shipbuilding, and other water cooling and treatment components [1-2]. Owing to its vast industrial applications and economic reasons, researchers have paid close attention to corrosion studies of aluminum and aluminum alloys. Al is an intrinsically active metal; it relies on a protective oxide film for stability [3]. The formed film dissolved in acidic or basic solutions has localized breakdown of the passive coating, which leads to the development and growth of corrosion pits. Several approaches, including corrosion inhibitors, are employed to address this issue. Various organic inhibitors have been used for resist aluminum corrosion [4-7]. Because of their toxicity, these inhibitors have not been strongly suggested. Plants extracts are also used as corrosion inhibitors and have good inhibition efficiency [8-11]. These natural inhibitors require separation of the extract into definite constituents in order to predict the binding sites, inhibition mechanism, etc. as well plant extracts are quite unstable and easily

degraded, which limits their use on industrial scales [12]. Last few years ionic liquids utilized by many researchers regard to low vapor pressure, high stability over wide range of pH and temperatures. [13-14]. So the aim of this study is to use the new three liquids based on imidazolium as green inhibitors for pitting corrosion of aluminum alloy (AA6061) in a saline-alkaline solution (1.0 M NaCl + 0.1M Na₂CO₃).

2. Materials and methods

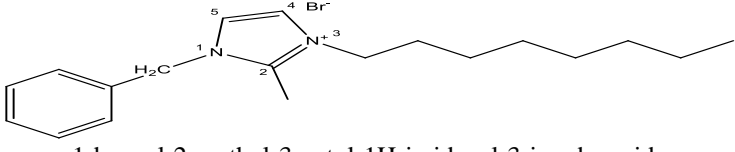
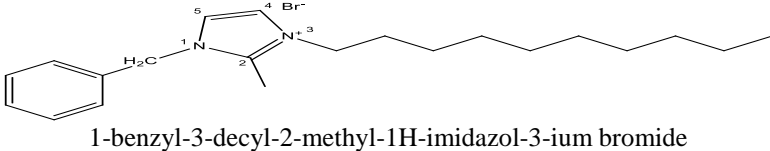
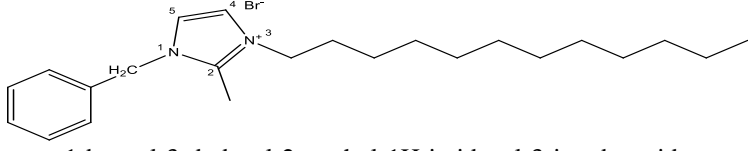
2.1. Materials and chemicals

Egyptian Petroleum Institute provided three unique synthetic ionic liquids that were employed as corrosion inhibitors. Table 1 contains the chemical formula as well as the names of the compounds.

Sodium chloride, and sodium carbonate (NaCl, Na₂CO₃) salts comes by Sigma Aldrich.

The CMRDI institute provided the aluminum alloy sheet AA6061 with content 0.92 percent Mg, 0.53 percent Si, 0.26 percent Cu, 0.15 percent Fe, and 96.4 percent Al make up this alloy.

Table 1. Chemical structures of tested inhibitors

Inhibitor Code	Molecular structures/Chemical name	Chemical Formula/ Molecular Weight
C8	 1-benzyl-2-methyl-3-octyl-1H-imidazol-3-ium bromide	C ₁₉ H ₂₉ BrN ₂ 365.36
C10	 1-benzyl-3-decyl-2-methyl-1H-imidazol-3-ium bromide	C ₂₁ H ₃₃ BrN ₂ 393.41
C12	 1-benzyl-3-dodecyl-2-methyl-1H-imidazol-3-ium bromide	C ₂₃ H ₃₇ BrN ₂ 421.47

2.2. Electrochemical tests

The palmSens potentiostat and the programme PStTrace5 version 5.7 were used in the electrochemical tests. Sweeping the potential in the forward way between -1600 and -200 mV versus Ag/AgCl using a scanning speed of 5.0 mV/s yielded the cyclic polarisation (CP) curves. Using the same sweep rate, the potential was then cycled in the negative direction. At open circuit settings, EIS tests were conducted in the frequency region between 0.01 Hz to 105 Hz using amplitude of 10 mV. At 298 K, electrochemical evaluations were carried out in a bottle with a volume of 50 ml, utilising a conventional 3 - electrode unit combination with Pt wire as the counter electrode, Ag/AgCl as the reference electrode, and sheet AA6061 as the working electrode. Before the studies, the AA6061 samples were manually abraded with various grades of silicon carbide papers (320 - 1200) until they had a mirror appearance, then cleaned with de-ionized water, and finally acetone.

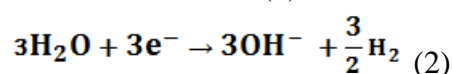
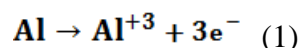
2.3. Surface Examination

Surface morphology of AA6061 specimens in different tested solutions was studied using scanning electron microscope (SEM) JOEL JSM-6510LV, Atomic-Force-Microscopy (AFM) (Park systems, model-XE-100) and XPS (ESCALAB 250 Xi (Thermo Fisher Scientific, USA)).

3. Results and Discussion

3.1. Cyclic potentiodynamic polarization:

Fig. 1 represents the CP curves of AA6061 electrode immersed in (1.0 M NaCl +0.1M Na₂CO₃) with different concentrations of ionic liquids (C12 as an example) inhibitors at 298K. From Fig.1 there is wide passive region of an oxide film of AA6061 electrode surface start from -1.6 to -0.8 V which formed by anodic reaction (metal oxidation) [15]. The deposition of solid oxide on the electrode surface occurs when the concentration of aluminum oxide at the anode surface reaches its solubility product, implying that the development of the passive layer proceeds through a dissolution precipitation process. The anodic current density reduces to a minimal value once the surface is completely coated with passive layer, signalling the start of passivation [16]. Prior to hydrogen evolution, the reverse cathodic response has one cathodic peak. It may be assumed that the diminution of the passive film is responsible for this peak. This passive film damaged in presence of corrosive medium and aggressive species like chloride ions [17].



Chloride ions present in solution react with Al in crystal lattice of oxide and form soluble oxy-chloride complex which enhances metal dissolution and accelerate presence of pits [18].



It is clear that by addition of ionic liquid inhibitors, pitting potential (E_{pit}) shifted to more positive potential value (see Table 1). Reduction in pitting sensitivity can be measured by increase in difference between E_{pit} and protection potential (E_{pro}) (i.e. $\Delta E = E_{\text{pit}} - E_{\text{pro}}$) (see Table 1), indicates that ionic liquid molecules adsorbed on the surface and as well as protect the surface from being pitted. The increase in the ΔE value in Fig. 1 is more abrupt until 150 ppm of ionic liquids (C8, C10, and C12). The related cathodic and anodic polarization curves display Tafel type behavior, as seen in Fig. 2.

Furthermore, the intersection of Tafel lines extrapolation yields the corrosion current density (i_{corr}) which is comparable to the corrosion rate. Table 2 summarizes the values of i_{corr} . According to the statistics, the following is the sequence in which the values of i_{corr} and hence the rate of corrosion decrease: C12 > C8 > C10. As the concentrations of the three ionic liquids rise, the rate of corrosion reduces. The optimal ionic liquid concentrations were approximately 150 ppm (C8, C10, and C12).

The addition of ionic liquids causes the value of corrosion potential E_{corr} to move towards less negative potentials (Table 2). This suggests that these inhibitors (C8, C10, and C12) have a strong influence on anodic processes (anodic inhibitors). This regarded that the corrosion of Al in 0.1M Na_2CO_3 +1.0 M NaCl solution inhibited by ionic liquids [19]. These findings imply that ionic liquids (C8, C10, and C12) adsorb at the Al/solution

interface to prevent general and pitting corrosion of aluminum in 0.1M Na_2CO_3 +1.0 M NaCl solution. Their imidazol-3-ium groups adsorb via an ion pair and exchange process, while their hydrophobic chains are directed towards the aqueous medium [20-22].

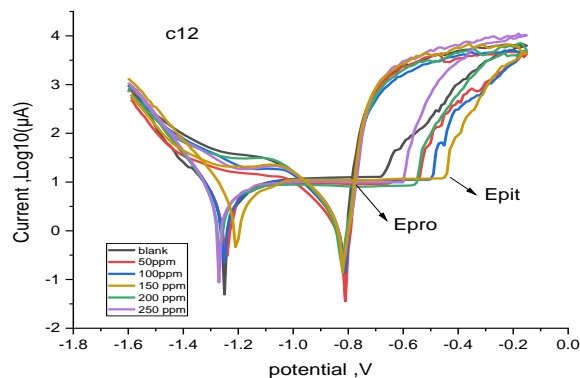


Fig. 1 CP curves of AA6061 electrode immersed in (1.0 M NaCl +0.1M Na_2CO_3) with different concentrations of ionic liquids (C12 as an example) inhibitors at 298K.

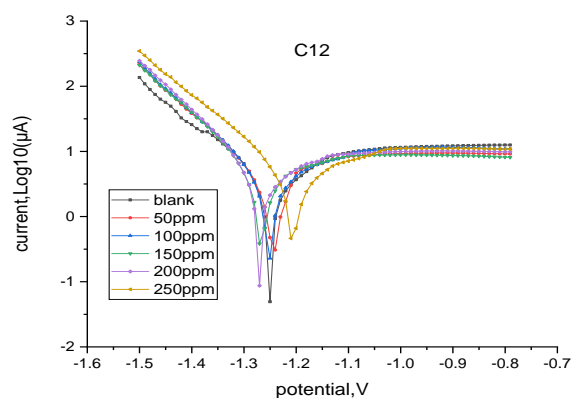


Fig. 2 Tafel type behavior of AA6061 electrode immersed in (1.0 M NaCl +0.1M Na_2CO_3) with different concentrations of ionic liquids (C12 as an example) inhibitors at 298K.

Table 2. Effect of different concentrations of ionic liquids inhibitors on corrosion parameters of AA6061 in (1M NaCl +0.1M Na_2CO_3) at 298K.

Inhibitors	[conc]ppm	E_{pit} V	E_{prot} V	E_{corr} V	i_{corr} $\mu\text{A cm}^{-2}$	ΔE
C12	0.0	-0.680	-0.788	-1.274	3.917	0.108
	50	-0.538	-0.773	-1.252	3.288	0.235
	100	-0.499	-0.773	-1.246	3.673	0.274
	150	0.438-	-0.771	-1.259	2.716	0.333
	200	-0.555	-0.771	-1.262	3.206	0.216
	250	-0.604	-0.766	-1.209	2.944	0.162
C10	50	-0.565	-0.787	-1.259	3.140	0.222
	100	-0.555	-0.780	1.248-	2.328	0.225
	150	0.531-	-0.771	-1.278	1.908	0.240
	200	-0.576	-0.773	-1.302	3.213	0.197
	250	-0.652	-0.780	-1.317	3.140	0.128
C8	50	-0.541	-0.780	-1.281	2.831	0.239
	100	-0.538	-0.78	-1.274	2.612	0.242
	150	0.439-	-0.771	-1.378	2.093	0.332
	200	-0.561	-0.781	-1.3607	3.639	0.220
	250	-0.591	-0.780	-1.356	3.443	0.189

3.2. AC Impedance spectroscopy (EIS)

To gather details on the surface passive layer on AA6061, an EIS study was performed in a 1 M NaCl+0.1 Na₂CO₃ solution without and with different dosages of ionic liquids (C8, C10, and C12). At 298 K, the relevant Impedance profiles are presented in Fig. 3. Each impedance graph, according to the data, has a wide capacitive circle during high frequencies (HF), a tiny inductive loop at middle frequencies (MF), and a 2nd capacitive looping during low frequencies (LF) (Fig. 3a). The relaxation mechanism in the aluminum oxide (or hydrated oxide) layer existing on the aluminum surface, as well as its dielectric characteristics, might be attributed to the HF capacitive looping. [23]. The dissolving of Al at low frequencies or the dissolution of the surface oxide layer has also been attributed to an inductive loop [24,25]. Inductive activity can be characterized by changes in surface area or salt film properties such as density, electrical properties, or depth [26]. With increasing ionic liquids (C8, C10, and C12) concentrations, the size of both HF and LF loops grew significantly. Three time-constants are seen in the Bode profiles (Fig. 3 b,c), notably two time-

constants with in HF and LF areas, and another time-constant mostly in MF region. An equivalent circuit style, as shown in Fig. 3d, is the ideal way to express the impedance results.

Solution resistor (R_s), inductance (L), inductance resistor (R_L), and charge transfer resistor (R_{ct1}) are all parallel to the double layer capacitance in the model (C_{dl1}). This circuit includes another (C_{dl2}) and (R_{ct2}). These values relate to the $Al^+ \rightarrow Al^{+3}$ reactions [27]. The total of R_{ct1} and R_{ct2} might reflect the polarization resistance, R_p . R_{ct} and R_p values rise dramatically with the injection of ionic liquids (C8, C10, and C12) leading to reduced electrode degradation (see Table 3) [28]. The findings in Table 3 illustrate that an increase in R_{ct1} and R_{ct2} values is related with a decrease in C_{dl1} and C_{dl2} over the entire range of concentrations. It is possible to argue that the ionic liquid molecules bonded on the AA6061 surface replace the water molecules at the AA6061 surface, resulting in a fall in C_{dl} values [29]. The rate of corrosion decreases as the concentrations of the three ionic liquids increase. The best ionic liquid concentrations were around 150 ppm (C8, C10, and C12).

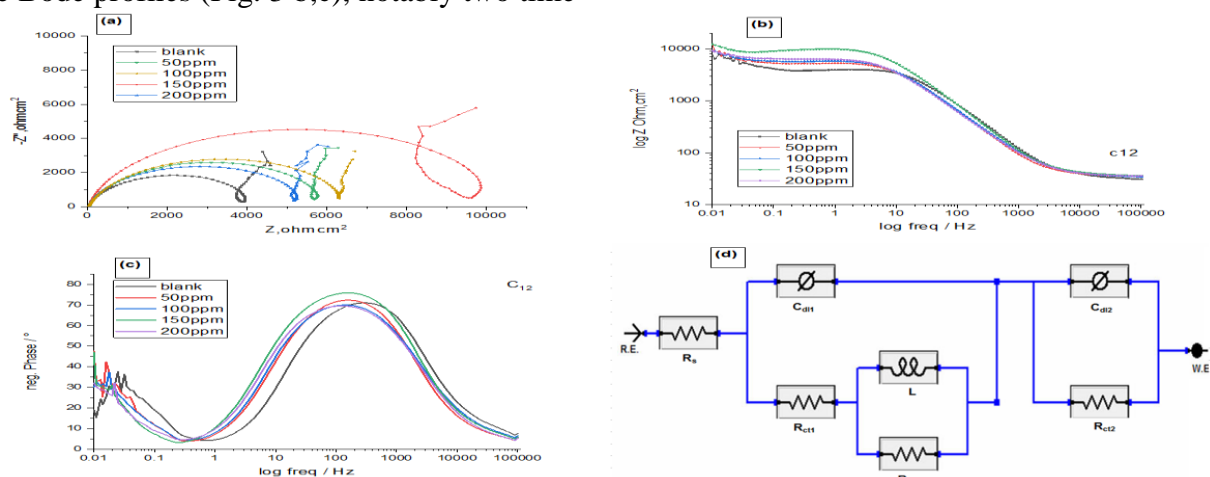


Fig. 3 Impedance spectra (a) Nyquist, (b) Bode-module (c) and Bode-phase angle plots, (d) equivalent circuit for of AA6061 electrode immersed in (1.0 M NaCl +0.1M Na₂CO₃) with different concentrations of ionic liquids (C12 as an example) inhibitors at 298K.

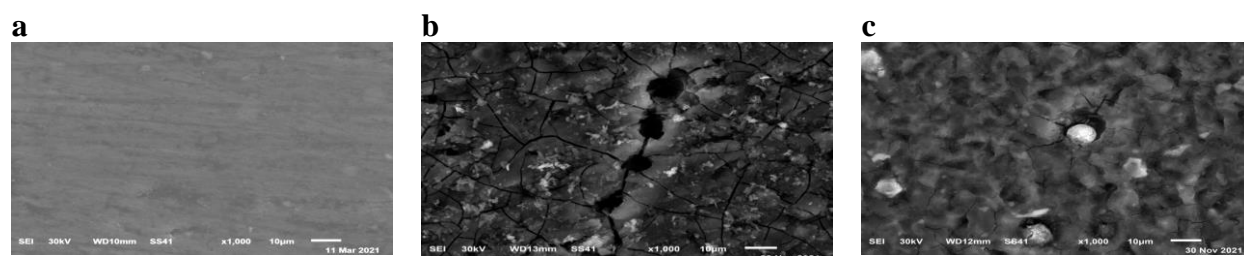


Fig. 4 SEM images of AA6061 (a) abraded, (b) after immersion in (1M NaCl +0.1M Na₂CO₃) (c) after immersion in (1M NaCl +0.1M Na₂CO₃ + 150 ionic liquid C12) at 298K

Table 3. Effect of different concentrations of ionic liquids inhibitors on EIS parameters of AA6061 in (1M NaCl +0.1M Na₂CO₃) at 298K.

Inhibitors	[conc]ppm	R _s Ω	R _{ct1} kΩ cm ²	C _{dl1} μF cm ⁻²	R _{ct2} Ω k cm ²	C _{dl2} μF cm ⁻²	R _{pk} Ω cm ²
C12	0.0	1.4	3.98	4.3	2.50	6.3	6.48
	50	1.1	4.89	4.1	3.38	5.4	8.37
	100	1.2	5.88	3.2	4.20	4.8	10.08
	150	1.1	6.34	2.9	4.98	3.0	11.32
	200	1.2	4.26	3.6	3.10	4.9	7.36
C10	50	1.1	5.32	3.7	3.25	5.3	8.57
	100	1.2	5.99	2.4	4.11	4.7	10.10
	150	1.2	8.32	1.3	4.53	4.2	12.86
	200	1.3	5.02	2.5	3.22	4.5	7.24
C8	50	1.2	5.21	2.7	3.05	5.9	8.21
	100	1.3	6.39	1.8	4.22	4.8	10.61
	150	1.4	9.98	0.6	4.67	3.6	14.65
	200	1.2V	5.19	2.9	2.98	5.0	8.17

3.3. Surface Morphology

SEM survey to estimate the surface morphology of AA6061 after 2 weeks immersion in (1M NaCl +0.1M Na₂CO₃) and (1M NaCl +0.1M Na₂CO₃ + 150 ionic liquid C12) solutions. Fig. 4 (a) shows and SEM image of a polished AA6061 with a relatively smooth surface. The photo in Fig. 4 (b) shows that the AA6061 surface is clearly cracked as a result of a strong attack on the corrosive medium without inhibitors also presence of pits. The cracks disappear and the surface of Al is smoother (Fig 4 c) than the surface of AA6061 in (1M NaCl +0.1M Na₂CO₃) without ionic liquids. This proves that the ionic liquids delays the corrosion of AA6061 by adsorbing the compound to the alloy surface. AFM is becoming an accepted method for investigation of the roughness of metals, and alloys. The three dimensional AFM image After keeping AA6061 in (1M NaCl +0.1M Na₂CO₃) for 24 h at 298 K (see Fig. 5 a) shows high surface roughness reach 318.13 nm, while in the presence of (1M NaCl +0.1M Na₂CO₃ + 150 ionic liquid C12) mixture it decreased to 99.578nm See Fig 5 (b). The decrease in average surface roughness of aluminum in presence of C12 is due to the adsorption of these ionic liquids on aluminum surface forming protective layer, so the metal surface became more smoothly and the corrosion rate was decreased.

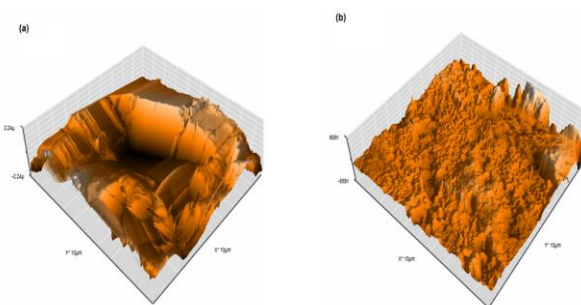


Fig. 5 AFM images of AA6061 (a) after immersion in (1M NaCl +0.1M Na₂CO₃) (b) after immersion in (1M NaCl +0.1M Na₂CO₃ + 150 ionic liquid C12) at 298K.

High resolution XPS spectra of AA6061 after immersion in (1M NaCl +0.1M Na₂CO₃) and (1M NaCl +0.1M Na₂CO₃ + 150 ionic liquid C12) are shown in Fig. 6 and 7, respectively. XPS spectrum of Al 2P has peak at 74.3 eV, which correspond to oxide peak of Al₂O₃ [30]. On the other hand, the Cl 2p signal can split into two peaks for samples at 198.02 and 199.39, which indicates that Cl⁻ anions had interacted with the substrate [31]. The C 1S spectra of aluminum in 1M NaCl +0.1 M Na₂CO₃ has three characteristic peaks at 286.27 eV and 287.94 eV and 289.2 eV which correspond to C-C C-O, and C=O respectively [32], there is other peak observed at 284.67 eV attributed to the SP² hybridized carbon come from ionic liquid C12. The O 1S show three peaks one of them at 531.7 eV and belonged to the metal oxide species. One peak at 1071.6 eV corresponding to Na₂CO₃. The N 1S peak at 401.1 eV was assigned to the coordinated nitrogen in the imidazolium ring with the surface of the AA6061 [33]. The appearance

peak of N in the inhibited sample surface confirmed the adsorption of ionic liquid C12

compounds on the AA6061 surface.

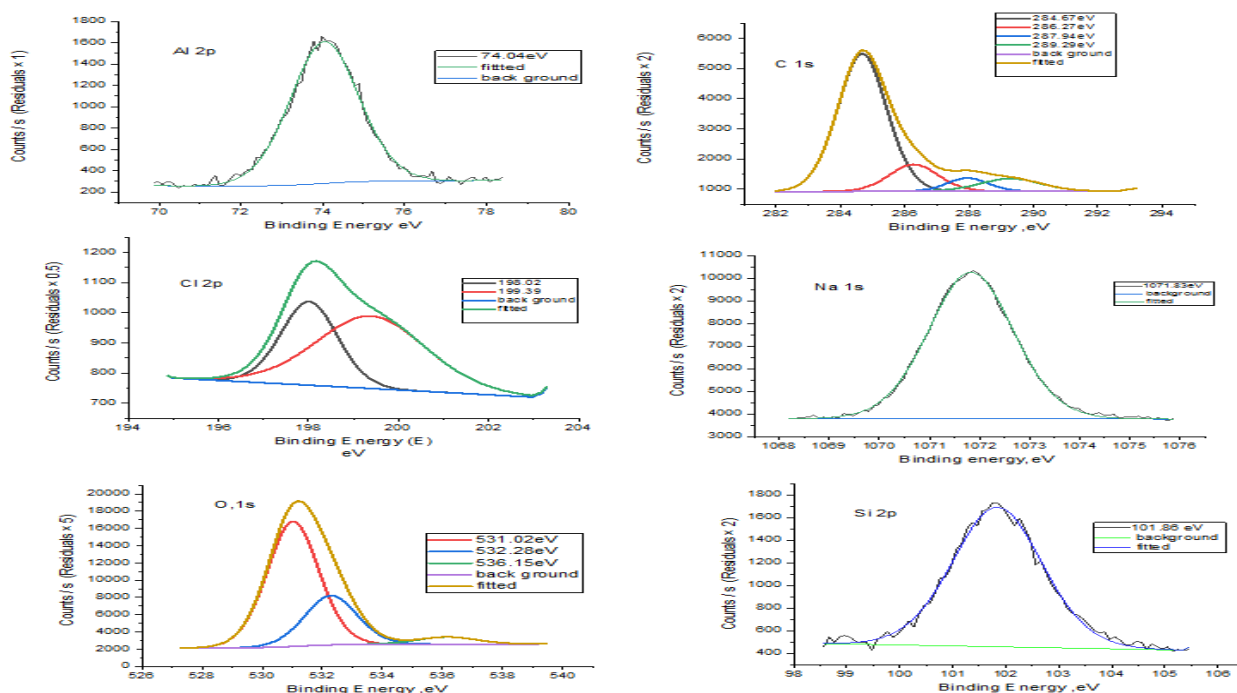


Fig. 6 High resolution XPS spectra of (Al 2P, O 1S, Cl 2P, C 1S, Na 1S ,Si 2P) for AA6061 after immersion in (1M NaCl +0.1M Na₂CO₃)

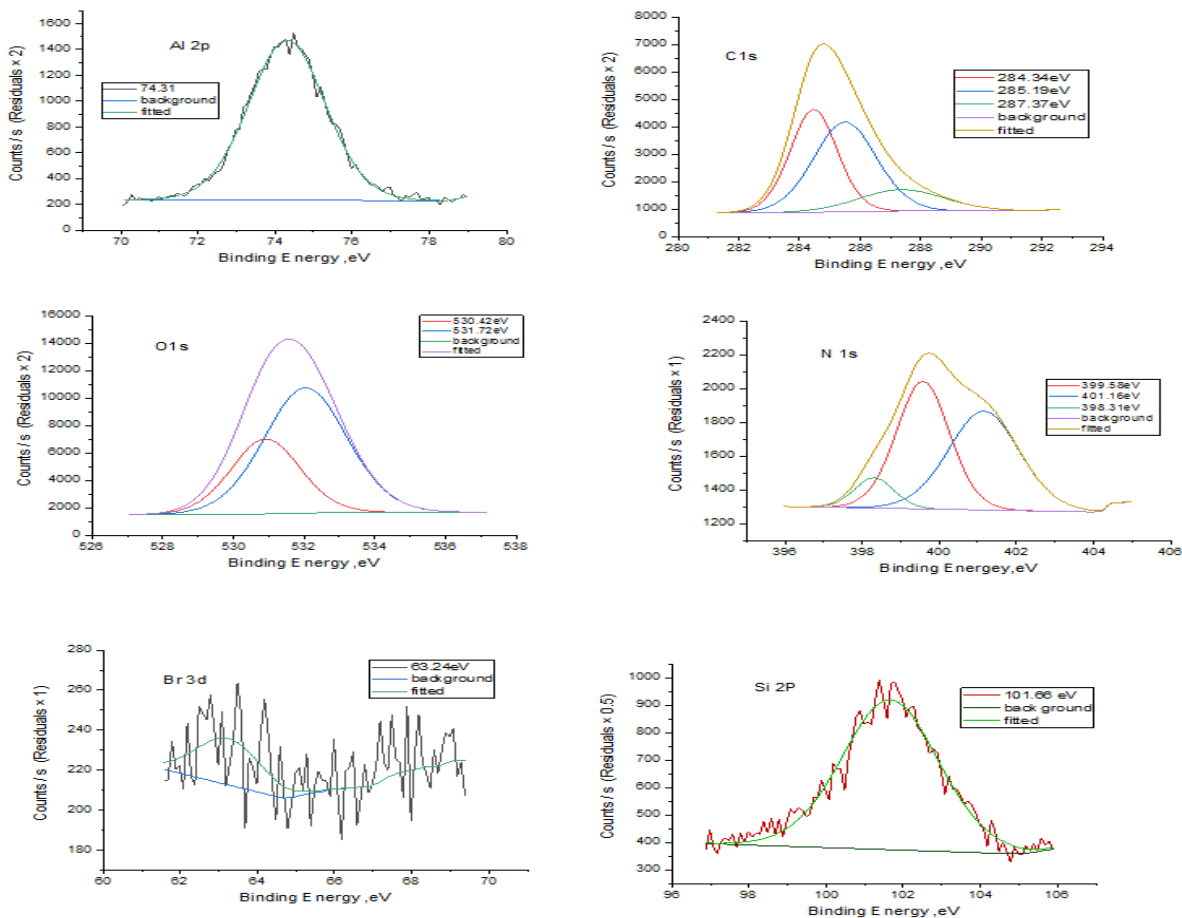


Fig. 7 High resolution XPS spectra of (Al 2P, O 1S, Cl 2P, C 1S, Na 1S, Si 2P, Br3d, N1S) for AA6061 after immersion in (1M NaCl +0.1M Na₂CO₃ + 150 ionic liquid C12) at 298K.

4. Conclusion

Three liquids based on imidazolium were investigated as green inhibitors for pitting corrosion of aluminum alloy (AA6061) in a saline-alkaline solution (1.0 M NaCl + 0.1M Na₂CO₃) in various experimental circumstances. It is clear that by addition of ionic liquid inhibitors, pitting potential (E_{pit}) shifted to more positive potential value. The ionic liquids molecules adsorbed on the surface and as well as protect the surface from being pitted. As the concentrations of the three ionic liquids rise, the rate of corrosion reduces. Both R_{ct} and R_p value increases significantly with addition of ionic liquids (C8, C10, and C12) due to slower corrosion of electrode. The optimal ionic liquid concentrations were approximately 150 ppm (C8, C10, and C12). According to SEM, AFM, and XPS experiments, ionic liquids postpone aluminum pitting corrosion by adsorbing the compound to the alloy surface.

4. References

1. B. Zhou, X. Wei, Y. Wang, Q. Huang, B. Hong, Y. Wei, (2019) Surf. Coat. Technol., 379, Article 125056
2. H. Li, P. Zhao, Z. Wang, Q. Mao, B. Fang, R. Song, Z. Zheng, Corros. Sci. (2016), 107 (jun.), pp. 113-122.
3. M.A. Deyab, (2019) Effect of nonionic surfactant as an electrolyte additive on the performance of aluminum-air battery, *Journal of Power Sources* **412** 520–526.
4. Hill J. A., Markely T., Forsyth M., Howlett P.C., Hinton B. R. W., (2011) corrosion inhibition of 7000 series aluminum alloys with cerium di phenyl phosphate, *J. alloy. Compd* , **509**, 1683-1690.
5. S. S. Abd El-Rehim, H. H. Hassan, M. A. Deyab, A. Abd El Moneim, (2016) Experimental and theoretical investigations of adsorption and inhibitive properties of Tween 80 on corrosion of aluminum alloy (A5754) in alkaline media, *Z. Phys. Chem.* **230** 67–78.
6. Khanariab K., Finšgar, M., (2016) Organic corrosion inhibitors for aluminium and its alloys in acid solutions:A review. *RSC Adv.*, **6**, 62833–62857.
7. Padash, R., Rahimi-Nasrabadi, M., Rad, A.S., Sobhani-Nasab, A., Jesionowski, T., Ehrlich, H., A (2019) theoretical study of two novel Schi_ bases as inhibitors of carbon steel corrosion in acidic medium. *Appl. Phys. A* , 125, 78.
8. Deng, S.D., Li, X.H., (2012) Inhibition by JasminumnudiflorumLindl leaves extract of the corrosion of aluminum in HCl solution. *Corros. Sci.* , **64**, 253–262.
9. S. Nofrizal, A.A. Rahim, B. Saad, P. Bothi Raja, A.M. Shah, S. Yahya (2012) Elucidation of the corrosion inhibition of mild steel in 1.0 M HCl by catechin monomers from commercial green tea extracts, *Metall. Mater. Trans. A Phys. Metall. Mater. Sci.*, **43**, pp. 1382-1393,
10. S.A. Asipita, M. Ismail, M.Z.A. Majid, Z.A. Majid, C. Abdullah, J. Mirza Green (2014) Bambusa Arundinacea leaves extract as a sustainable corrosion inhibitor in steel reinforced *concrete J. Clean. Prod.*, **67**, pp. 139-146
11. P.B. Raja, M.G. Sethuraman, Natural products as corrosion inhibitor for metals in corrosive media - a review *Mater. Lett.*, **62** (2008), pp. 113-116
12. Palou, R.M., Olivares-Xomelt, O., Likhanova, N.V., (2014) Environmentally Friendly Corrosion Inhibitors. In *Development in Corrosion Protection*; IntechOpen: London, UK, , 431–465.
13. Arellanes-lozada P., Olivares O., Guzman-lucero D., Likhanova N.V., Dominiguez Aguilar M.A., (2014) Liganova I.V, Elasa Arece-Estrada, *Materals* , **7**, 5711-5734.
14. M.A. Deyab, (2018) Ionic liquid as an electrolyte additive for high performance lead-acid batteries, *Journal of Power Sources* **390** 176–180.
15. E.E.Foad El-Sherbini, S.M.Abd El-Wahab and M.A.Deyab, (2006) Electrochemical behavior of tin in sodium borate solutions and the effect of halide ions and some inorganic inhibitors. *Corrosion science journal*, **48** 1885-1898.
16. M.A. Deyab, (2009) The influence of different variables on the electrochemical behavior of mild steel in circulating cooling water containing aggressive anionic species. *Journal of Solid State*

- Electrochemistry* **13** 1737-1742.
17. Chen, H.; Chow, C.L.; Lau, D. (2022) Deterioration Mechanisms and Advanced Inspection Technologies of Aluminum Windows. *Materials*, **15**, 354.
 18. McCafferty, E. (2003) Sequence of Steps in the Pitting of Aluminum by Chloride Ions. *Corros. Sci.*, **45**, 1421–1438.
 19. Su-II Pyun á Sung-Mo Moon, (2000) Corrosion mechanism of pure aluminium in aqueous alkaline solution, *J. Solid State Electrochem.*, **4**, 267-272.
 20. M.A. Deyab, (2018) Efficiency of cationic surfactant as microbial corrosion inhibitor for carbon steel in oilfield saline water, *Journal of Molecular Liquids* **255** 550–555.
 21. M.A. Deyab S.S. Abd El-Rehim, (2012) On surfactant-polymer association and its effect on the corrosion behaviour of carbon steel in cyclohexane propionic acid. *Corrosion science journal* **65** 309–316.
 22. M.A. Deyab, (2017) 1-Allyl-3-methylimidazolium bis(trifluoromethylsulfonyl)imide as an effective organic additive in aluminum-air battery, *Electrochimica Acta* **244** 178–183.
 23. M.A. Deyab, Amr A. Nada, A. Hamdy, (2017) Comparative study on the corrosion and mechanical properties of nano-composite coatings incorporated with TiO₂ nano-particles, TiO₂ nano-tubes and ZnO nano-flowers, *Progress in Organic Coatings* **105** 245–251.
 24. Abd El Rehim, S.S., Hassan, H.H., Amin, M.A., (2001) Corrosion inhibition of aluminum by 1,1(lauryl amido) propylammonium chloride in HCl solution. *Mat. Chem. Phys.*, **70**, 64–72.
 25. M.A. Deyab, Najlae Hamdi, Mohammed Lachkar, B. El Bali, (2018) Clay/Phosphate/Epoxy nanocomposites for enhanced coating activity towards corrosion resistance, *Progress in Organic Coatings* **123** 232–237
 26. Bessone J. B., Salinas D. R., Mayer C. E., Ebert M., Lorenz W.J. (1992), An EIS study of aluminium barrier-type oxide films formed in different media. *Electrochim. Acta.*, **37**, 2283–2290.
 27. Al-Kharafi FM, Badawy WA (1998) Inhibition of corrosion of Al 6061, aluminum, and an aluminum-copper alloy in chloride-free aqueous media: Part 2- Behavior in basic solutions. *Corrosion* **54**:377–385.
 28. F. El-Taib Heakal, M.A. Deyab, M.M. Osman, M.I. Nessim, A.E. Elkholy, (2017) Synthesis and assessment of new cationic Gemini surfactants as inhibitors for carbon steel corrosion in oilfield water, *RSC Advances* **7** 47335-47352.
 29. Ansari KR, Quraishi MA (2014) Bis-Schiff bases of isatin as new and environmentally benign corrosion inhibitor for mild steel. *J Ind Eng Chem* **20**:2819–2829.
 30. R. Tamilarasan, A. Sreekanth, (2013) Spectroscopic and DFT investigations on the corrosion inhibition behavior of tris (5-methyl-2-thioxo-1,3,4-thiadiazole) borate on high carbon steel and aluminium in HCl media, *RSC Adv.*, **3** 23681–23691.
 31. P. Arellanes-Lozada, O. Olivares-Xomet, N.V. Likhanova, J.R. Vargas-García, R.E. (2018) Hernández-Ramírez, Adsorption and performance of ammonium-based ionic liquids as corrosion inhibitors of steel, *J. Mol. Liq.*, **265** 151–163.
 32. H. Piao, N.S. (2002) McIntyre, Adventitious carbon growth on aluminium and gold-aluminium alloy surfaces, *Surf. Interface Anal.*, **33** 591–594.
 33. M. Lagrenee, B. Mernari, M. Bouanis, M. Traisnel, F. Bentiss, (2002) Study of the mechanism and inhibiting efficiency of 3,5-bis(4-methylthiophenyl)-4H-1,2,4-triazole on mild steel corrosion in acidic media, *Corros. Sci.*, **44** 573–588.